Mechanistic study of methane reforming with carbon dioxide on a supported nickel catalyst

Yan Zi-Feng*, Qian Ling, Liu Xin-Mei, Song Lin-Hua, Song Chun-Min, Ding Rong-Gang, Yuan An and Qiao Ke

State Key Laboratory of Heavy Oil Processing, PetroChina Key Laboratory of Catalysis, China University of Petroleum, Dongying 257061, China

The nature of activation of methane on supported nickel catalyst has been investigated by means of temperature programmed surface reaction (TPSR), temperature programmed desorption (TPD), X-ray photoelectron energy spectroscopy (XPS) and pulse reaction and a synergetic mechanism of carbon dioxide reforming with methane is tentatively postulated. TPSR, TPD and XPS results indicate that carbidic C_α, carbonaceous C_β and carbidic clusters C_γ surface carbon species formed by decomposition of methane show different surface mobility, thermal stability and reactivity. C_α and C_β species on the nickel surface are thermally unstable and can be rapidly converted into C_γ species upon increasing temperature. The carbidic carbon is a very active and important intermediate in carbon dioxide reforming with methane and the carbidic clusters C_γ species might be the precursor of the surface carbon deposition.

Keywords: carbon dioxide reforming with methane, supported nickel catalyst, methane activation, surface carbonaceous species, synergetic mechanism

During the past decades, the process of carbon dioxide reforming with methane has received attention. Efforts have focused on development of catalysts that show high activity towards synthesis gas formation, and are also resistant to carbon formation, thus displaying stable long-term operation. Within the design of a potential catalyst, nickel is envisioned as the optimum active component. Carbon deposition is a fatal problem to nickel-based catalysts in the dry reforming process. Nowadays, two viewpoints have been proposed about the mechanism of carbon dioxide reforming with methane. The general opinion is that first methane is adsorbed, activated, and dissociated on the reduced metal catalyst. Nevertheless, dispute occurs about whether carbon dioxide also dissociates on the surface of the catalyst. Takayasu[1] suggested that gaseous carbon dioxide directly reacts with dihydrogen formed from methane and water, steam reforming then follows to obtain synthesis gas. That is to say, the substance of the carbon dioxide reforming is the same as the steam reforming.

To elucidate the reaction mechanism, a deeper understanding of the kinetic characteristics of the carbon dioxide reforming reaction is necessary. The reported typical kinetic models for CH_4/CO_2 reforming reaction are listed in Table 1. The gaseous phase non-catalytic results are somewhat inadequate to explain the true catalytic carbon dioxide reforming process. In spite of that, the activation energy values of elementary steps clearly indicate that pure methane decomposition has to overcome a high energy barrier, while carbon dioxide dissociation is more difficult than is methane. However, there is a much lower activation energy for the reaction between carbon dioxide with H or CH_x fragments.

Davidson[2] (model 1) suggested that gaseous carbon dioxide directly reacts with H_2 formed from methane and water, steam reforming then follows to obtain synthesis gas. Thus the partial pressure of water is very important for dry reforming of methane.

Bodrov[3,4] (model 2) considered that the mechanism of carbon dioxide reforming is consistent with that of steam reforming, which is rather similar to the viewpoint proposed by Takayasu.[1] Model 1 and 2 mean that steam reforming might be crucial for dry reforming reaction of methane and the partial pressure of water could bean indicator of the extent of the dry reforming reaction.

* Correspondent. E-mail: zfyancat@hdpu.edu.cn

Table 1 Reported kinetic models for CH_4/CO_2 reforming reaction

No	Model	Catalyst	ref.
1	$r=\frac{kP_{CH_4}(P_{CO_2}+P_{H_2O})}{[1+24(P_{CO_2}+P_{H_2O})+8P_{H_2}]^2}$	Cu/SiO_2	[2]
2	$r=\frac{kP_{CH_4}}{1+a\frac{P_{H_2O}}{P_{H_2}}+bP_{CO}}$	Ni foil	[4]
3	$r=\frac{k_R K_{CO_2} K_{CH_4} P_{CH_4} P_{CO_2}}{(1+K_{CO_2}P_{CO_2}+K_{CH_4}P_{CH_4})^2}$	Rh/Al_2O_3	[8,9]
4	$r=\frac{aP_{CH_4}P_{CO_2}^2}{(P_{CO_2}+bP_{CO_2}^2+cP_{CH_4})^2}$	Ni/Al_2O_3 $Ni/CaO\text{-}Al_2O_3$	[7]

The kinetic model 3 was suggested based on the L-H mechanism plus redox mechanism.[5] Zhang[6,7] proposed the kinetic model 4 according to the L-H mechanism and considered methane decomposition the rate determining step. Models 3 and 4 argued over whether carbon dioxide dissociates during the reforming reaction on the surface of the catalyst.

The stepwise dehydrogenation of methane to CH_x fragments is widely accepted, but it needs to be established whether carbon dioxide only reacts with H_2 formed by methane decomposition. The ready reaction between carbon dioxide with CH_x fragments occurs. The results, which were derived from the direct detection of laser spectra, may be credible.

Some researchers considered the rate-determining step of the methane decomposition is the difficult C–H rupture, whose energy barrier is as high as 435kJ/mol. But, as a matter of fact, it is not like that. The activation of methane is really difficult in a reaction system like oxidation coupling of methane, which employs a metal oxide catalyst. A very high temperature is necessary (usually above 1050K) and the activation of methane may be the rate-determining step of the overall reaction. However, the activation of methane on a supported metal catalysts is not very difficult. Erdöhelyi[8] reported studies of the decomposition of methane on a supported Rh catalyst employing temperature-programmed reduction and pulse reaction technology. The results indicated

that methane might decompose even at 423K. His *in situ* IR spectra studies indicated that pure carbon dioxide might dissociate on a Rh/Al_2O_3 catalyst above 523K.

The reaction of methyl species on Ni(111) and Ni(100) was studied[10] employing mass spectroscopy. The results showed that the C–H rupture of methyl readily occurs at 220 K. This appears to be good evidence that C–H rupture of a fairly stable methyl is easy. As mentioned above, the activation of methane on group VIII metals is not very difficult. The strong chemisorption of CH_x and dihydrogen formed by methane on metals may largely decrease the energy barrier of dehydrogenation of methane and promotes its stepwise dissociation at lower temperature. Compared with group VIII metals, metal oxide catalysts do not have strong interaction with methane and CH_x, so very high temperature is necessary for the activation of methane to supply enough energy.

Erdöhelyi *et al.*[11] proposed a mechanism of carbon dioxide reforming with methane over supported noble metal catalysts on the basis of kinetic studies. Methane may undergo two reactions with the following routes: stepwise dehydrogenation, followed by surface reaction with surface oxygen or OH to CO and H_2; firstly direct reaction with surface oxygen species to CH_x, thereafter following the former route. Carbon dioxide may react with adsorbed hydrogen, surface carbon and surface CH_x fragments.

The mechanism of carbon dioxide reforming with methane may change somewhat when a different type of catalyst is used. Zhang and Verykios[12] reported that a Ni/La_2O_3 catalyst showed high stability because a new reaction pathway occurred at the Ni/La_2O_3 interface. They proposed a mechanism that under the CO_2/CH_4 reaction conditions, CH_4 mainly cracks on the Ni crystallites to form H_2 and surface carbon species (CH_x species), while CO_2 preferably adsorbs on the La_2O_3 support or the LaO_x species which are decorating the Ni crystallites in the form of $La_2O_2CO_3$. At high temperatures the oxygen species of $La_2O_2CO_3$ may participate in reactions with the surface carbon species (CH_x) on the neighbouring Ni sites to form CO. Due to the existence of such synergetic sites which consist of Ni and La elements, the carbon species formed on the Ni sites are favorably removed by the oxygen species originated from $La_2O_2CO_3$, thus resulting in an active and stable performance.

Temperature-programmed oxidation experiments have been conducted employing isotope labeled $^{13}CH_4$ over a Rh/Al_2O_3 catalyst in the carbon dioxide reforming system.[13] The results showed that carbon deposition on the catalyst primarily derives from carbon dioxide and to a lesser extent from methane. The reported mechanism of carbon dioxide reforming cannot explain this fact reasonably. Further studies are necessary for elucidation of the detailed reaction pathway and mechanism.

In this paper, our purpose is to investigate the nature of activation of methane on a supported nickel catalyst by means of TPSR, TPD, XPS and pulse reaction and find a way to illustrate the possible mechanism of carbon dioxide reforming with methane. Such an endeavour might be feasible for commercialisation of dry reforming of methane in the future.

Experimental

Catalyst preparation

The supported nickel catalysts were prepared by a conventionally incipient wetness impregnation method, with aqueous solutions of nitrates as promoter and metal precursors.[14] The 20–40 mesh support, γ-Al_2O_3 (Qilu Catalyst Work, Sinopec.), was calcined for 6 h at 773 K in air before the catalyst preparation. The saturated water holding capacities of the pretreated supports were measured. The residues were dried overnight in air at 373 K, subsequently followed by calcination in air at 523 K for 0.5 h, 673 K for 0.5 h, and 873 K for 6 h for complete decomposition of the nitrate.

Catalysts used in this study included 8wt% Ni/Al_2O_3 s (unpromoted), 10wt% Ni/Al_2O_3 (unpromoted) and 10wt% Ni-2wt%MgO/Al_2O_3 (promoted).

All reagents used in catalyst preparation are A.R.-grade chemicals produced in China.

Catalyst characterisation

Catalyst pretreatment

The catalyst sample (100mg) was first pretreated in an O_2 flow of 20 ml/min at 973K for 30 min, then the O_2 flow was switched to an H_2 flow of 30 ml/min for 1h. After the sample was cooled to room temperature in an H_2 flow, a 30 ml/min He flow was introduced to purge the sample for 30 min.

Temperature programmed surface reaction (TPSR)

TPR, TPD, TPSR and pulse reaction experiments were carried out in an apparatus, which consisted of a flow switching system, a heated reactor, and an analysis system (Fig. 1).

TPSR experiments were also performed in the quartz-fixed-bed micro-reactor at a constant heating rate (20K/min). A 20 ml/min flow of methane was continually pulsed into the catalyst at a certain temperature stated in the text and then the reactor was quickly cooled to ambient temperature. Subsequently, a 30 ml/min flow of H_2/He (1:2) or CO_2/He (1:10) was introduced to flush the reactor continuously to take away the mixture of gases and physically adsorbed species. After that treatment, the surface intermediate species produced in the reforming process were well characterised by TPSR in the mixed gas flow. The desorbed species from the metal surface along with the temperature-programmed process were simultaneously detected by the *on-line* DYCOR quadrupole mass spectrometer. All gases used in TPSR experiments are of the purity of 99.99%.

Temperature programmed desorption (TPD)

TPD experiments were conducted at a constant heating rate (23K/min), using ultra high purity helium as carrier gas, at a flow rate of 30 ml/min. When the required adsorption temperature was reached, the helium flow was switched to CO, CO_2 or CH_4 flow. The tested gas was adsorbed on the sample for 30 min. The He flow was switched again to flush the reactor after cooling to room temperature in the adsorption gas flow. Then temperature programming was initiated and the analysis of the desorbed gases was performed with an *on-line* quadrupole mass spectrometer (DYCOR Quadrupole, Ametek Instrument). In the TPD process, the helium gas was dried with $[Mg(ClO_4)_2]$ and deoxygenated with 402 deoxygenating reagent. The residual oxygen in the carrier gas that flowed over the catalyst was removed by a cold trap of liquid nitrogen before flowing into the reactor. Leak tests on the reaction system were also strictly performed to exclude the possibility of the oxidation of surface carbon.

X-ray photoelectron energy spectroscopy (XPS)

XPS for nickel samples was conducted on a VG ESCALAB 210 X-ray photoelectron spectrometer with Mg Kα radiation and a base pressure of 10^{-8}Pa. The specially designed pretreatment cell made sure that during transfer, the XPS sample was not exposed to air before XPS experiments. The Si_{2p} level, with a binding energy of 102.7e V, was used to correct the charge effect as the reference line. The Fisons Eclipse Data System was used to perform the data acquisition and analysis.

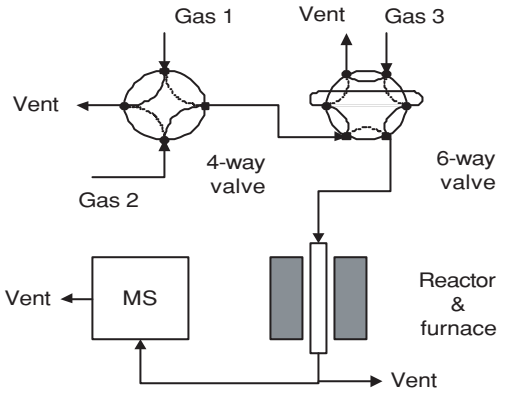

Fig. 1 Schematic of the transient response kinetic analysis system.

Pulse reactions

The pulse reaction experiments were conducted in the quartz fixed-bed reactor following the catalysts pretreatment. Methane was pulsed continually on the pretreated catalysts using high purity helium as carrier gas at 973K. Subsequently, a 20 ml/min flow of H_2/He (1:2) or CO_2/He (1:10) mixture was introduced to flush the reactor continuously to take away the gaseous and physically adsorbed mixture. Then TPSR was initiated in the flow of H_2/He (1:2) or CO_2/He (1:10) at a heating rate of 23 K/min. When the temperature was increased to 973K, the carrier gas was switched again, then, 0.39 ml of H_2, CO_2, or O_2 were continually pulsed respectively into the micro-reactor under high temperature. The desorbed products from the metal surface were simultaneously detected by the *on-line* DYCOR quadrupole mass spectrometer.

Results and discussion

Carbon dioxide reforming had been proposed by Fischer and Tropsch as a substitute for the steam reforming process and most of the group VIII metals, except Os, were more or less effective for catalysis of carbon dioxide reforming with methane.[15] The noble metal catalysts exhibited promising performance for the reforming reaction. Ashcroft[16] examined the stoichiometric carbon dioxide reforming reaction at 1050K and atmospheric pressure and achieved 90% yield of synthesis gas without carbon-free formation on Ru, Rh and Ir. Furthermore, Ru and Rh showed high selectivity for carbon-free operation. The sequence of activity for carbon dioxide reforming reaction or carbon-free formation was Ru, Rh > Ir > Ni, Pt, Pd.[17] Loadings of metals on supports also affect the activity of the catalysts. Low loadings (about 1–5%) of the noble metals are usually sufficient because of their effective performance.[16] Higher loadings are required for Ni and Co catalysts in which the metal-support interactions are stronger than in the case of heavier metals.

Carbon deposition over catalysts is the fatal problem for carbon dioxide reforming with methane.[18-24] Although some noble metals show high activity and selectivity for carbon-free operation, high cost and limited availability of noble metals prevent the commercial use of this reaction. It is, therefore, more practical to develop an improved nickel-based catalyst which exhibits stable operation for a long period of time.

TPR investigation of nickel catalyst

Fig. 2a showed the temperature programmed reduction profiles of NiO, unpromoted and promoted catalysts. The deconvoluted TPR profile of NiO exhibited the existence of two kinds of primary nickel oxide crystalline phase at 670 K and 735 K, respectively. The amount of H_2 consumption of the latter peak was much more than that of the former one. The response of H_2O intensity lagged behind that of H_2 due to a large quantity of water formation in the TPR process.

Figs 2b and 2c indicate that appropriate promoter addition and decreased calcination temperature may be a good solution for prohibiting the formation of the $NiAl_2O_4$ spinnel phase, which appeared at 1040K. Addition of strong basic MgO significantly affected the basicity/acidity of the support, leading to a profound change in the bulk phase composition. It was observed that while the reduction peak of $NiAl_2O_4$ phase was significantly reduced, that of NiO was greatly enhanced (Fig. 2a). This was ascribed to the fact that the basic MgO was preferably reacting with the acid Al_2O_3 to form stable magnesium aluminate, thereby suppressing the reaction between NiO and Al_2O_3. The decreased reduction temperature of NiO and prohibition of formation of $NiAl_2O_4$ phase were obtained on the catalyst with an appropriate addition amount of MgO promoter. This gives a partial explanation for the optimum catalytic performance of the MgO- promoted nickel catalyst.

Fig. 3 showed that NiO reduction peaks disappeared and a new reduction peak at 1040 K appeared on the unpromoted catalyst. This peak may be attributed to the reduction of the $NiAl_2O_4$ spinnel phase. The higher calcination temperature (973 K) may be responsible for the formation of the $NiAl_2O_4$ spinnel phase in the Ni/Al_2O_3 catalyst. The formation of the $NiAl_2O_4$ spinnel phase results from the solid reaction between NiO and the acidic Al_2O_3 support at high calcination temperature. $NiAl_2O_4$ spinnel phase is rather difficult reduce, as witnessed by the fact that it essentially survives H_2 reduction at 1000 K.[6] Therefore, less $NiAl_2O_4$ spinnel phase can be reduced to nickel metal active sites in the H_2 flow at 973 K. As a result, this catalyst provided low activity for carbon dioxide reforming reaction.

TPSR studies

Methane decomposition on transition metal surface is a thermally assisted, catalytic activated process. In this study, several questions are addressed. First, how do carbonaceous fragments, in particular the simplest fragment-$CH_{x(ad)}$ species, bond to metal surfaces with more complex structure than that to single crystal surfaces? Secondly, a low-index nickel single crystal surface should be effective toward the decomposition of methane, but can an alumina-supported nickel catalyst surface be effective in the decomposition of methane? What is the mechanism of thermal decomposition of methane on alumina-supported nickel catalysts? The TPSR, TPD, and XPS techniques are used to identify surface-bound species and gas-phase products of decomposition of methane adsorbed on alumina-supported nickel catalysts.

For the reaction of CO_2 reforming with methane, the most probable slow steps are methane activation to $CH_{x(ad)}$ ($x = 0 \sim 3$) species, and the reaction between $CH_{x(ad)}$ species and the oxidant, either in the form of oxygen adatoms originated from CO_2 dissociation or CO_2 itself. The *on-line* quadrapole mass spectroscopy and ion-trap experiments have confirmed that methane promotes the dissociation of carbon dioxide on the catalysts. The promotion of carbon dioxide is attributed to the effect of dihydrogen formed in the decomposition of methane. It seems that the key to elucidation of the nature of the CO_2 reforming with methane over $Ni/\gamma\text{-}Al_2O_3$ catalyst is to derive a mechanistic scheme of activation and dissociation of methane.

A great effort was made to detect adsorbed carbonaceous $CH_{x(ad)}$ fragments formed in the decomposition of methane by means of sensitive *in situ* FT–IR spectroscopy. However, no adsorption bands attributable to any vibration modes of carbonaceous $CH_{x(ad)}$ species were identified either by *in situ* measurements or after a sudden cooling of the sample in a continuous methane flow at 700 K. This means that carbonaceous $CH_{x(ad)}$ species react or decompose too

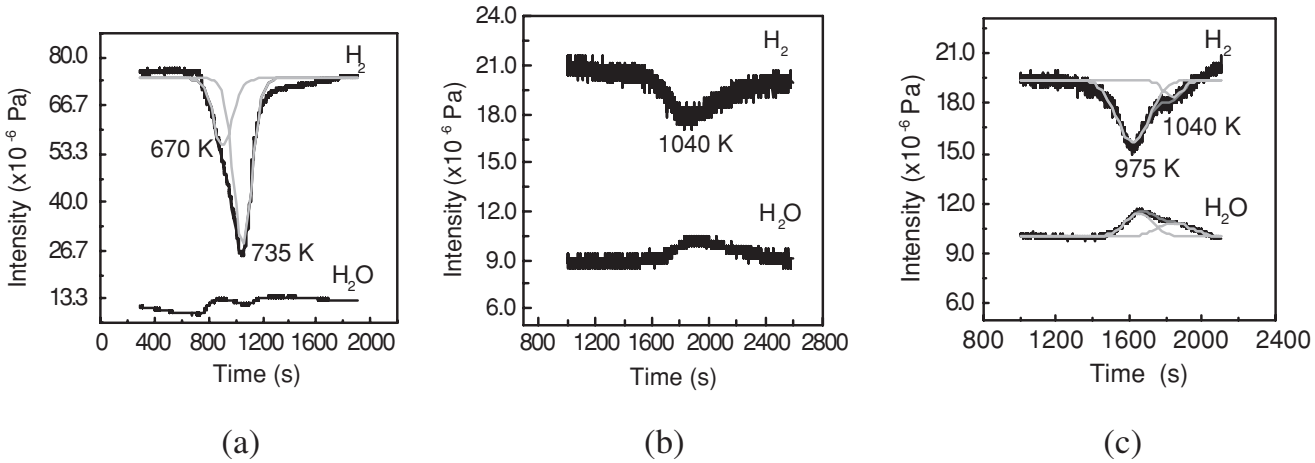

Fig. 2 TPR profiles of NiO prepared by calcination at 873 K. (a) NiO; (b) 10wt% Ni/Al_2O_3 catalyst (unpromoted); (c) 10wt% Ni–2wt%MgO/Al_2O_3 catalyst (promoted).

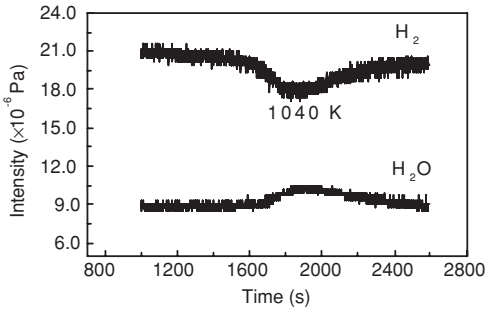

Fig. 3 TPR profiles of 10wt% Ni/Al_2O_3 catalyst (unpromoted) calcined at 973 K.

quickly at high temperature, or their surface concentrations are below the detection limit.

However, the presence of surface carbonaceous $CH_{x(ad)}$ species was well manifested by their reaction with dihydrogen. After flushing the reactor with H_2/He (1:2) flow (following methane decomposition at a certain temperature), the hydrogenation of the surface carbonaceous $CH_{x(ad)}$ species was investigated by TPSR technique. Fig. 4 showed that the decomposition of methane could result in the formation of at least three kinds of surface carbon species on an 8wt% Ni/Al_2O_3 catalyst. Generally, the carbon deposition is comprised of various forms of carbon that are different in terms of reactivity. The distribution and features of these carbonaceous species depend sensitively on the nature of transition metals and the conditions of methane adsorption. These carbonaceous species can be described as: completely dehydrogenated carbidic (C_α type), partially dehydrogenated CH_x ($1 \le x \le 3$) species, namely the C_β type, and carbidic clusters (C_γ type) formed by the agglomeration and conversion of C_α and C_β species under certain conditions. A fraction of the surface carbon species, which might be assigned to carbidic C_α (~461 K), was mainly hydrogenated to methane even below 500 K. This showed that the carbidic C_α species is rather active and thermally unstable on the nickel surface. The carbidic C_α species has already been suggested to be responsible for CO formation.[25] A significant amount

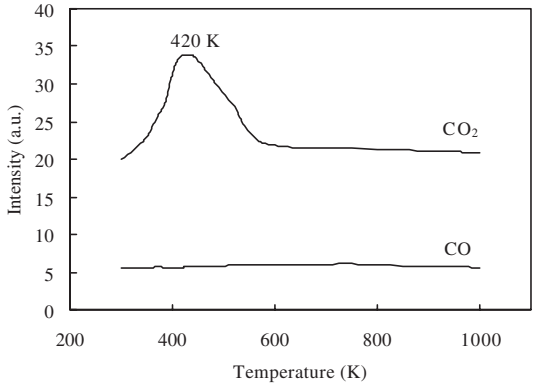

Fig. 5 CO_2 TPD over fresh 8wt% Ni/Al_2O_3 catalyst.

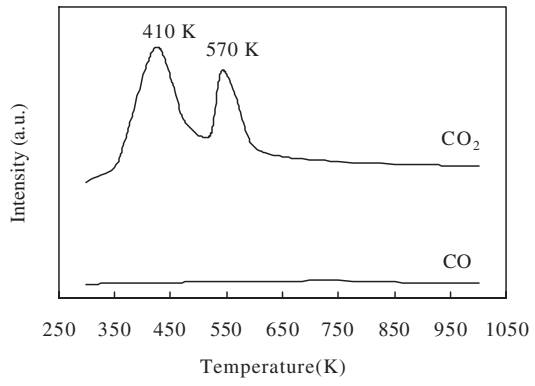

Fig. 6 CO TPD over fresh 8wt% Ni/Al_2O_3 catalyst.

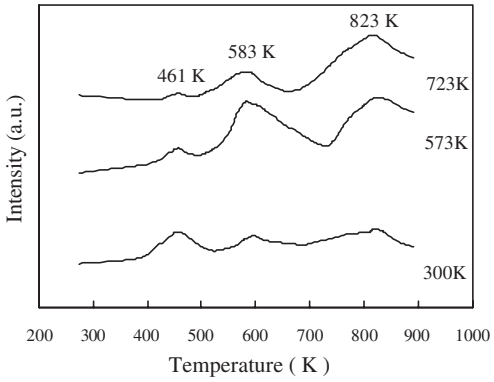

Fig. 4 TPSR spectra of CH_4/He pulsed at different temperatures (or 300 K, 573 K and 723 K) then cooled and reheated in H_2/He flow on fresh 8wt% Ni/Al_2O_3 catalyst.

of surface carbon species was hydrogenated to methane below 600 K and was assigned to partially dehydrogenated C_β (~583 K) species. The majority of the surface carbon was hydrogenated above 800 K and was attributed to carbidic clusters C_γ (~823 K).[25]

Fig. 4 also indicates that the formation of three kinds of surface carbon species with different structures and properties largely depends on the exposure temperature and duration of exposure to methane. When the nickel catalyst was exposed to methane above 723 K, the carbidic C_α species was not detected, and a significant amount of C_β was transformed into the carbidic clusters C_γ. This indicates that the carbidic clusters C_γ species might be the precursor of the surface carbon deposition, which may be produced by the interactions between C_α and C_β species, and/or between C_α species, and/or between C_β species themselves.

TPD elucidation

CO_2 TPD

Fig. 5 shows CO_2 TPD on fresh 8 wt% Ni/Al_2O_3 catalyst after pretreatment. CO_2 was adsorbed on the catalyst at room temperature (300 K). A broad CO_2 desorption peak appeared at 420 K on the CO_2 TPD profiles and very little CO desorption was detected. This suggests that CO_2 is weakly adsorbed on the catalyst and only a kind of adsorption state of CO_2 is formed. From the thermodynamic point of view, dissociative adsorption of CO_2 is rather difficult on the reduced 8wt% Ni/Al_2O_3 catalyst. Hereby, it is reasonable that very little CO_2 dissociation was observed from TPD profiles.

CO TPD

The CO TPD profiles over the fresh Ni/Al_2O_3 catalyst were obtained following CO adsorption at 300 K (Fig. 6). The rate of CO_2 formation was recorded to monitor the occurrence of CO disproportionation during the process of temperature programming. It was observed that two apparent CO_2 desorption peaks appeared at 410 K and 570 K, but the intensity of CO remained almost unchanged. The CO_2 desorption peak at 410 K was similar to the CO_2 peak on the CO_2 TPD profiles, which desorbed at 420 K. Thus it appears that the CO disproportionation reaction occurred at room temperature and weakly adsorbed

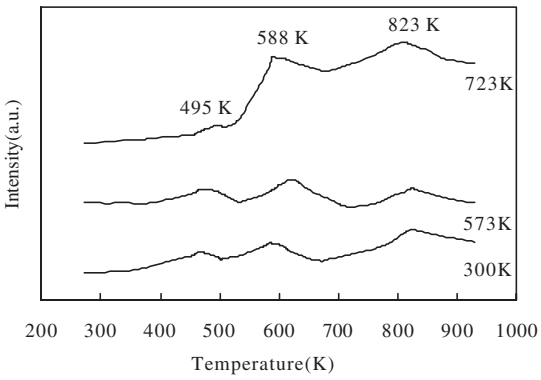

Fig. 7 TPD spectra of CH_4 in He flow on fresh 8wt% Ni/Al_2O_3 catalyst at different temperatures.

CO_2 was formed. The CO_2 desorption at 570 K may be derived from disproportionation of strongly adsorbed CO on the catalyst.

CH_4 TPD

As shown in Fig. 7, TPD spectra of methane on fresh Ni/Al_2O_3 catalyst show three corespondent peaks of CO_2. Thus methane decomposition on transition metals truly takes place and the reactivity of the surface carbon species depends sensitively on the variables of the reactions.

For TPSR spectra in a flow of dihydrogen, desorbed products were mainly methane (Fig. 4). But for TPD spectra in a flow of helium, the desorbed species were mainly CO_2 and some CO, which means that the TPD process is actually a process of temperature-programmed oxidation (TPO), in which the surface carbon is oxidised to form CO and CO_2. The surface oxygen species, which resulted in the oxidation of surface carbon, might be the residual or remaining surface bonded oxygen (M–O) on transition metals. The oxygen atoms in the subsurface and bulk phase of the metal cannot migrate to the surface below 1000 K.[10] The TPD results in Fig. 7 indicate that the surface residue oxygen species after *in-situ* reduction might be irreducible and very different to migrate on the surface. It also means that the desorbed species should result from the interaction between mobile carbonaceous species and immobile residual oxygen species on the catalyst surface. Furthermore, XPS results showed that the crystalline alumina support does not interact with the surface carbon at moderate temperature (< 850 K). Thus, the CO and CO_2 produced during the TPD process might originate from the partially reduced oxygen bonded to the transition metal. This kind of bonded oxygen is rather difficult to be reduced under the pretreatment conditions and cannot migrate from one site to another. It also meant that the residual NiO_x species dispersed on the surface of 8wt% Ni/Al_2O_3 catalyst were stepwise reduced during the reaction.

During the TPD process, the surface carbon produced by the decomposition of methane might migrate to the sites of bonded oxygen and interact with them to form carbon oxides. This means that the peak temperature gaps (ΔT) of corresponding surface carbon species between TPD and TPSR might be the parameters for characterising the mobility of the different surface carbon species (Figs 4 and 7). An examination of the peak temperature gap indicated that the mobility of different surface carbon species on the nickel catalyst is consistent with the order $C_\gamma > C_\alpha > C_\beta$, with the ΔT values of 0, 5, and 34 K, respectively. This indicates that the carbonaceous species formed by the decomposition of methane are sufficiently mobile to interact with partial metal oxide to form CO_2. In the meantime, from Fig. 7 another conclusion can be drawn that C_α and C_β species can be transformed into C_γ species and the transformation could be accelerated by the increasing adsorption temperature, similar to the data exhibited in TPSR studies (Fig. 4).

XPS determination

The XPS experiments and Ar^+ etching techniques could give more supporting information. The binding energy data of the catalyst calcined in air at 973 K, reduced in H_2 at 973 K and exposed to methane followed by reduction were obtained by XPS experiments. The results showed that surface nickel exists in an oxidised state (B.E. 856.00 eV) for the calcined sample, a partially oxidised state (B.E. 853.64 eV) for reduced 8wt% Ni/Al_2O_3 sample in H_2 and in the metallic state (B.E. 852.90 eV) for the methane exposed sample (Fig. 8a). The binding energy of Ni metal is 852.30 eV, thus the catalyst exposed to methane following reduction exists essentially in the metallic state. This is also consistent with the CH_4 TPD results above (Fig. 7). That is to say, the residual NiO_x species dispersed on the surface of 8wt% Ni/Al_2O_3 catalyst can be stepwise reduced during the reaction.

XPS results showed that methane decomposition on 8wt% Ni/Al_2O_3 catalyst can result in three different types of surface carbon, similar to the TPSR results, whose binding energy are 282.00, 282.90 and 284.70 eV, respectively. The deconvoluted XPS spectra of C(1s) of 673 K-adsorbed CH_4 after sputtering by Ar^+ at 300 K are shown in Fig. 8b. Comparison of deconvoluted XPS spectra before and after Ar^+ etching indicates that C_α (B.E. 282.00 eV) and C_β (B.E. 282.90 eV) species are thermally unstable and can be transformed into C_γ species (B.E. 284.70 eV) under the experimental conditions.

Pulse reaction studies

First, CO_2 TPSR was performed in the mixed gas of CO_2/He (1:10) following CH_4 pulses over a reduced 8wt% Ni/Al_2O_3 catalyst

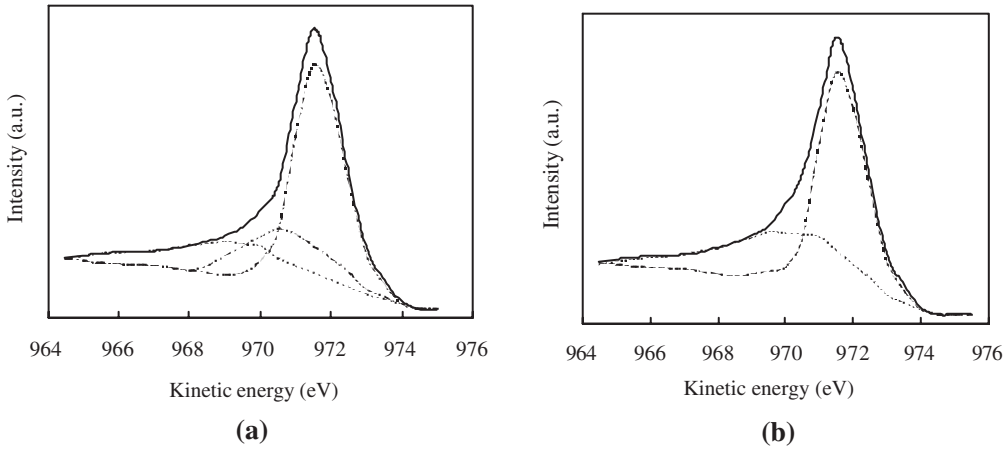

Fig. 8 Deconvoluted XPS of C(1s) of 673K-adsorbed CH_4 at 300K. (a) before and (b) after sputtered by Ar^+ ions of 1.36×10^{-4} Pa at 300 K and 5 kV for 5 min.

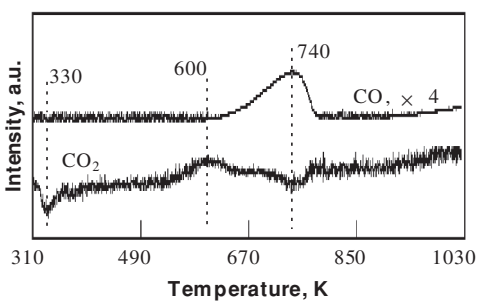

Fig. 9 TPSR in CO_2/He (1:10) following CH_4 pulses at 973K over reduced 8 wt% Ni/Al_2O_3 catalyst.

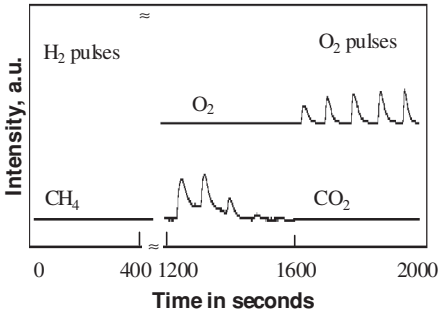

Fig. 10 H_2 and O_2 pulses patterns at 973 K following CO_2 TPSR over 8 wt% Ni/Al_2O_3 catalyst.

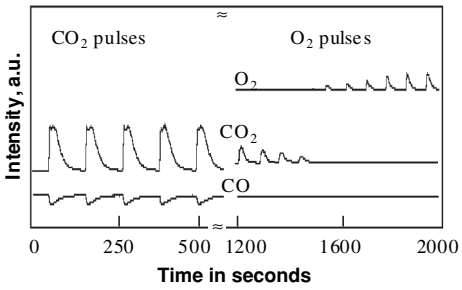

Fig. 11 CO_2 and O_2 pulses patterns at 973 K after H_2 TPSR over 8 wt% Ni/Al_2O_3 catalyst.

(Fig. 9), then the H_2 or O_2 pulse was introduced into the reactor (Fig. 10). In the same way, H_2-TPSR was performed in a mixed gas flow of H_2/He (1:2) following CH_4 pulses over reduced 8wt% Ni/Al_2O_3 catalyst, then the CO_2 or O_2 pulse was introduced into the reactor (Fig. 11).

Fig. 9 illustrates that a fraction of the CO_2 adsorbed on the catalyst at about 300 K and desorbed above 600 K in the CO_2/He flow. The equilibrium between the surface-adsorbed CO_2 and gaseous CO_2 was responsible for the higher CO_2 desorption temperature than that in He flow (420 K). The formation and desorption of CO could be observed while the surface CO_2 began to desorb greatly. The consumption of CO_2 and formation of CO reached a maximum at the increased temperature of 740 K. CO_2 TPSR on the Ni catalyst may suggest the reaction pathway of CO_2: it is first adsorbed on the surface of the catalyst, then reacts with neighbouring surface carbonaceous species to form CO. This is similar to the inference from the TPD experiment with the used catalyst as shown in Fig. 6.

The formation of CH_4 was not detected in the H_2 pulse reaction following CO_2 TPSR at 973 K. Fig. 10 shows that the surface carbonaceous species that could react with CO_2 were used up. Fig. 11 indicates that the formation of CO was not detected in the CO_2 pulse reaction following H_2 TPSR at 973 K, either. This means that the surface carbonaceous species which can react with H_2 were also used up. This type of surface carbonaceous species was active and can react with not only CO_2 but also with H_2. At the same time, other inert carbonaceous species may exist on the surface of the catalyst. The O_2 pulse reaction was continually carried out following the H_2 or CO_2 pulse reaction in order to verify the existence of other carbonaceous species (Fig. 11). The appearance of CO_2 pulses was good evidence for the existence of the other carbonaceous species, which were unable to react with H_2 or CO_2. The catalyst deactivation may result from the deposited carbon species that only react with O_2 at very high temperature.

Fig. 4 indicates the emergence of at least three kinds of surface carbonaceous species produced by the decomposition of methane at lower temperature. When the catalyst was exposed to methane at 973 K, the carbidic C_α species was completely converted into C_β or C_γ species. The partially dehydrogenated C_β species can react with H_2 or CO_2 to form CH_4 or CO, but the less active carbidic clusters C_γ species cannot react with H_2 or CO_2, but reacts with O_2 at high temperature. The H_2 and CO_2 TPSR and pulse reaction provide mutual verification of the existence and properties of the surface carbonaceous species.

Pulse reaction studies of CO_2 activation

At present, two viewpoints have been proposed about the mechanism of carbon dioxide reforming with methane. The general opinion is that first methane adsorbed, activated, and dissociated on the reduced metal catalyst. Herein, the role of CO_2 and the nature of CO_2 activation were investigated by means of a long pulse reaction method.

Fig. 12 indicates that carbon dioxide was actually decomposed into CO and carbidic species, which were hydrogenated to form methane, after introducing CO_2 flow for 7 min over fresh Ni/Al_2O_3 catalyst. But such a decomposition of CO_2 was hindered by the considerable formation of methane, which is adsorbed competitively on nickel sites, after subsequenlyt introducing a CO_2 flow for 12 min. At that moment, the CO_2-decomposed nickel catalyst was outgassed with argon flow and the only product was a little hydrogen. Subsequently, CO was produced after introducing a methane flow for 6 min. This means that the surface oxygen species produced by CO_2 decomposition could interact with the injected methane to form CO and some CO_2, but most of the CO_2 might be desorbed from the nickel sites while introducing methane. Thus the adsorption and activation

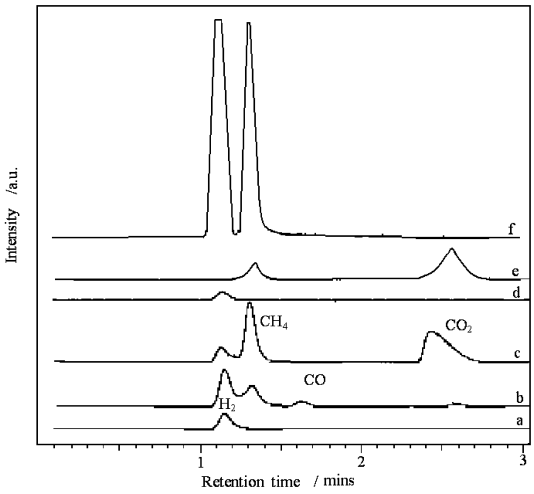

Fig. 12 CO_2 pulses patterns at 973 K over reduced Ni/Al_2O_3 catalyst: (a) After outgassing fresh catalyst with argon for 7 h; (b) After introducing CO_2 flow for 7 min and, (c) After introducing CO_2 flow for 12 mins and then; (d) After outgassing fresh catalyst with argon for 45 mins, subsequently, e) after introducing methane flow for 6 mins and then f) after introducing methane flow for 10 min.

of methane on nickel sites should be stronger than that of carbon dioxide in coexistence with methane and CO_2. It also appears that CO_2 actually decomposed to form CO_{ads}, C_{ads} and O_{ads} species on the fresh nickel surface. With the introducing of methane, the surface reaction might mainly be decomposition of methane and a large amount of hydrogen is produced. Therefore nearly all of the surface oxygen would be exhausted in such circumstance. The activation and decomposition of methane is crucial for reforming reaction and the surface carbonaceous species are mainly produced by decomposition of methane, during which CO_2 might greatly interact with surface carbonaceous species to form CO.

Based on all the above studies, it appearsa that the decomposition of methane on a supported nickel catalyst could result in the formation of at least three kinds of surface carbon species. Generally, the carbon deposition is comprised of various forms of carbon that are different in terms of reactivity. The distribution and features of these carbonaceous species depend sensitively on the nature of the transition metals and the conditions of methane adsorption. These carbonaceous species can be described as: completely dehydrogenated carbidic C_α type, partially dehydrogenated CH_x ($1 \le x \le 3$) species, namely C_β type, and carbidic clusters C_γ type formed by the agglomeration and conversion of C_α and C_β species under certain conditions. A fraction of the surface carbon species, which might be assigned to carbidic C_α (~461K), was mainly hydrogenated to methane even below 500 Thus the carbidic C_α species is rather active and thermally unstable on the nickel surface. The carbidic C_α species is suggested to be responsible for CO formation. The significant amount of surface carbon species that was hydrogenated to methane below 600K is assigned to partially dehydrogenated C_β (~583K) species. The majority of the surface carbon was hydrogenated above 800K and was attributed to carbidic clusters C_γ (~823K). The possible reaction processes of carbon dioxide reforming with methane was inferred as follows: methane is first decomposed into hydrogen and different surface carbon species, then the adsorbed CO_2 reacts with surface carbons to form CO.

The proposed mechanism is as follows:

(1) Dissociative adsorption of methane is the rate-determing step.

$$CH_{4(g)} \Leftrightarrow CH_{4(ad)} \Leftrightarrow CH_{x(ad)} + (4-x)H_{(ad)} \Leftrightarrow Carbon_{(ad)} + xH_{(ad)} \quad (x = 1 \sim 3)$$

(2) Dissociative adsorption of carbon dioxide

$$CO_{2(g)} \Leftrightarrow CO_{2(ad)} \Leftrightarrow CO_{(ad)} + O_{(ad)} \Leftrightarrow Carbon_{(ad)} + O_{(ad)}$$

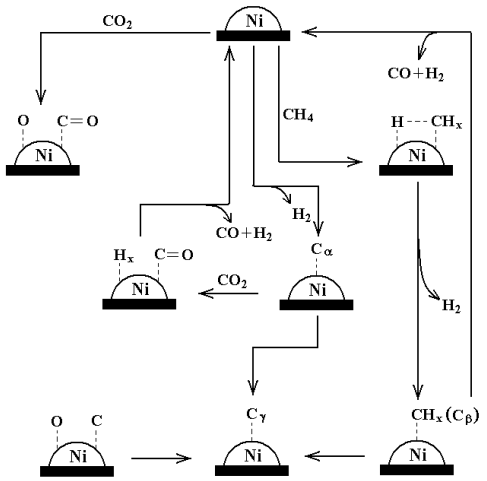

Fig. 13 Patterns of activation and reaction of methane with carbon dioxide on nickel catalyst.

(3) Formation of water

$$2H_{(ad)} + O_{(ad)} \Leftrightarrow H_2O_{(ad)} \Leftrightarrow H_2O_{(g)}$$

(4) Formation of hydrogen

$$2H_{(ad)} \Leftrightarrow H_{2(ad)} \Leftrightarrow H_{2(g)}$$

(5) Formation of carbon monoxide and decarbonation

$$CO_{(ad)} \Leftrightarrow CO_{(g)};\ Carbon_{(ad)} + O_{(ad)} \Leftrightarrow CO_{(ad)} \Leftrightarrow CO_{(g)}$$

Herein, $Carbon_{(ad)}$ means the carbidic C_α species, and $CH_{x(ad)}$ the carbonaceous C_β species.

The mechanism of reaction of surface carbons should be as follows:

$$C_\alpha + \ldots + C_\alpha \rightarrow C_\gamma$$
$$C_\beta + \ldots + C_\beta \rightarrow C_\gamma$$
$$C_\alpha + \ldots + C_\beta \rightarrow C_\gamma$$

Actually, such conversion of surface carbon species results in carbon deposition and made the catalyst deactivation.

This mechanism is actually the synergetic decomposition process of methane and carbon dioxide (described by Fig. 13).

Reforming with the optimum combination of oxidising agents, steam, carbon dioxide, and oxygen, is a very effective route to synthesis gas when better understanding of steam reforming is achieved. This makes the indirect conversion of methane a strong alternative to the new direct conversion processes. Based on the above discussion, dry reforming with methane shows several advantages compared with the steam reforming–methanation process. The disadvantage is the carbon deposition under certain conditions. Therefore, if the catalyst deactivation can be successfully resolved, the process can be rapidly commercialised. This means that the reaction of methane reforming with carbon dioxide is very promising from both industry and environmental protection points of view. Optimisation of dry reforming with methane would result in an industrial process to utilise natural gas and mitigate greenhouse emission.

Conclusions

CO_2 TPD showed that CO_2 weakly adsorbs on the catalyst and only a kind of adsorption state of CO_2 is formed. CO TPD indicated two kinds of adsorption states of CO exist on the catalyst and are desorbed in the form of CO_2 at different temperatures by CO disproportionation reaction.

Carbidic C_α, carbonaceous C_β and carbidic clusters C_γ surface carbon species, mainly formed by decomposition of methane, showed different surface mobility, thermal stability and reactivity. C_α and C_β species on the nickel surface are thermally unstable and can be rapidly converted into C_γ species upon increasing the temperature. The carbidic carbon is a very active and important intermediate in carbon dioxide reforming with methane and the carbidic clusters C_γ species might be the precursor of surface carbon deposition.

The CH_4 TPD process actually undergoes a TPO process involving the surface residual oxygen species. CO and CO_2 produced during the TPD process might originate from the partially reduced residual oxygen bonded to the transition metal. The residual partial oxidative NiO_x species that are not thoroughly reduced cannot migrate on the catalyst surface and can be stepwise reduced during the reaction.

The partially dehydrogenated C_β species can react with H_2 or CO_2 to form CH_4 or CO, but the less active carbidic clusters C_γ species cannot react with H_2 or CO_2, but react with O_2 at high temperature. The catalyst deactivation may result from the deposited carbon species that only react with O_2 even at very high temperature.

Based on all the above studies,a possible synergetic reaction mechanism of carbon dioxide reforming with methane is inferred and the pattern of activation and reaction of methane with carbon dioxide on the supported nickel catalysts is tentatively proposed.

This program was financially supported by Shandong Foundation of Excellent Young Scientists (SDYSF 97040826) and Innovation Foundation of Excellent Young Scientists (CNPC 40338200), PetroChina Co.

Received 13 December 2004; accepted 14 March 2005
Paper 04/2931

References

1 O. Takayasu, I. Matsuura, *Proc.10th ICC*, Budapest, 1992, p.1951.
2 D.F. Davidson, M.D.D. Rosa, E.J. Chang, R.K. Hanson and C.T. Bowman, *Int. J. Chem. Kinet.*, 1996, **28**, 171.
3 N.M. Bodrov and L.O. Apelbaum, *Kinet. Catal.*, 1967, **8**, 326.
4 W.K. Lewis, E.R. Gilliland and W.A. Reed, *Ind. Eng. Chem.*, 1949, **41**, 1227.
5 N.M. Bodrov and L.O. Apel'baum, *Kinet. Catal.*, 1967, **8**, 326.
6 Z.L. Zhang, X.E. Verykios, S.M. MacDonald and S. Affrossman, *J. Phys. Chem.*, 1996, **100**, 744.
7 Z. Zhang and X.E. Verykios, *J. Chem. Soc. Chem. Commun.*, 1995, 71.
8 A. Erdöhelyi, J. Cserényi and F. Solymosi, *J. Catal.*, 1993, **141**, 287.
9 A. Erdöhelyi, J. Cserenyi, E. Papp and F. Solymosi, *Appl. Catal.*, 1994, **108**, 205.
10 R.B. Hall, M. Castro, C.M. Kim and C.A. Mims, *Proc. 11th ICC*, Elsevier Science, Baltimore, July, 1996, USA.
11 A. Erdöhelyi, J. Cserényi and F. Solymosi, *J Catal.*, 1993, **141**, 287.
12 Z. Zhang and X.E. Verykois, *Catal. Today*, 1994, **21**, 589.
13 Z. Zhang and X.E. Verykios, *Catal. Today*, 1994, **21**, 589-595.
14 Z. Yan, R. Ding, L. Song and L. Qian, *Energy Fuels*, 1998, **12**, 1114.
15 V.F. Fischer and H. Tropsch, *Brennst. Chem.*, 1928, **3**, 39.
16 A.T. Ashcroft, A.K. Cheethan, M.L.H. Green and P.D.F. Vernom, *Nature*, 1991, **352**, 225.
17 J.R. Rostrup-Nielsen and J.H.B. Hansen, *J. Catal.*, 1993, **144**, 38.
18 A.M. Gadalla and B. Bower, *Chem. Eng. Sci.*, 1989, **43**, 3049.
19 A. Guerrero-Ruiz, A. Sepúveda-Escribano and I. Rodríguez-Ramos, *Catal. Today*, 1994, **21**, 545.
20 J.A. Lercher, J.H. Bitter, W. Hally, W. Niessen and K. Seshan, *Proc. 11th ICC*, Elsevier Science, July, 1996, Baltimore, USA.
21 Z. Zhang and X.E. Verykios, *Catal. Today*, 1994, **21**, 589.
22 A. Sacco, F.W.A.H. Geurts, J.A. Jablonski, S. Lee and R.A. Gately, *J. Catal.*, 1989, **119**, 322.
23 M.F. Mark and W.F. Maier, *Angew. Chem., Int. Ed. Engl.*, 1993, **33**, 1657.
24 Z. Zhang and X.E. Verykios, *Appl. Catal.*, 1996, **138**, 109.
25 Z. Zhang, X.E. Verykios, S.M. Macdonald and S. Affrossman, *J. Phys. Chem.*, 1996, **100**, 744.